AD-A169 780 THE DEVELOPMENT OF A CARS (COHERENT ANTI-STOKES RAMAN SPECTROSCOPY) SYSTE..(U) ARMY BALLISTIC RESEARCH LAB ABERDEEN PROVING GROUND MD R B PETERSON ET AL. JUN 86 1/1

UNCLASSIFIED BRL-TR-2734 F/G 7/4 NL

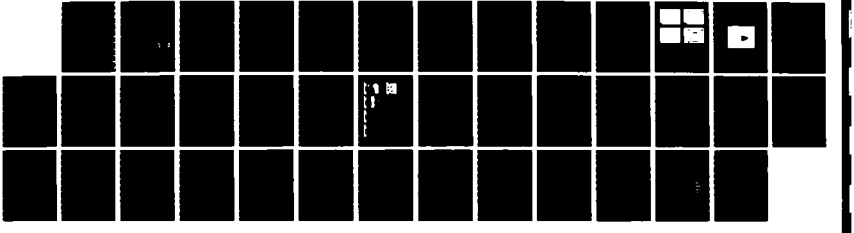

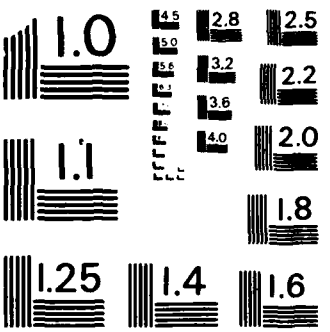

(12)

AD

US ARMY
MATERIEL
COMMAND

TECHNICAL REPORT BRL-TR-2734

THE DEVELOPMENT OF A CARS SYSTEM FOR THE STUDY OF MUZZLE FLASH

Richard B. Peterson
John A. Vanderhoff

June 1986

US ARMY BALLISTIC RESEARCH LABORATORY
ABERDEEN PROVING GROUND, MARYLAND

86

Destroy this report when it is no longer needed.
Do not return it to the originator.

Additional copies of this report may be obtained from the National Technical Information Service, U. S. Department of Commerce, Springfield, Virginia 22161.

The findings in this report are not to be construed as an official Department of the Army position, unless so designated by other authorized documents.

The use of trade names or manufacturers' names in this report does not constitute indorsement of any commercial product.

UNCLASSIFIED

SECURITY CLASSIFICATION OF THIS PAGE (When Data Entered)

REPORT DOCUMENTATION PAGE

READ INSTRUCTIONS BEFORE COMPLETING FORM

1. REPORT NUMBER: Technical Report BRL-TR-2734
2. GOVT ACCESSION NO.:
3. RECIPIENT'S CATALOG NUMBER:

4. TITLE (and Subtitle): THE DEVELOPMENT OF A CARS SYSTEM FOR THE STUDY OF MUZZLE FLASH

5. TYPE OF REPORT & PERIOD COVERED: Final

6. PERFORMING ORG. REPORT NUMBER:

7. AUTHOR(s): Richard B. Peterson*
John A. Vanderhoff

8. CONTRACT OR GRANT NUMBER(s):

9. PERFORMING ORGANIZATION NAME AND ADDRESS: US Army Ballistic Research Laboratory
ATTN: SLCBR-IB
Aberdeen Proving Ground, MD 21005-5066

10. PROGRAM ELEMENT, PROJECT, TASK AREA & WORK UNIT NUMBERS: 1L161102AH43

11. CONTROLLING OFFICE NAME AND ADDRESS: US Army Ballistic Research Laboratory
ATTN: SLCBR-DD-T
Aberdeen Proving Ground, MD 21005-5066

12. REPORT DATE: June 1986

13. NUMBER OF PAGES: 36

14. MONITORING AGENCY NAME & ADDRESS (if different from Controlling Office):

15. SECURITY CLASS. (this report): Unclassified

15a. DECLASSIFICATION/DOWNGRADING SCHEDULE: NA

16. DISTRIBUTION STATEMENT (of this Report):
Approved for Public Release; Distribution Unlimited.

17. DISTRIBUTION STATEMENT (of the abstract entered in Block 20, if different from Report)

18. SUPPLEMENTARY NOTES:
*Oregon State University
Corvallis, Oregon

19. KEY WORDS (Continue on reverse side if necessary and identify by block number)
Muzzle Flash
CARS
Flow Field
Carbon Monoxide
Spectroscopy

20. ABSTRACT (Continue on reverse side if necessary and identify by block number) meg

The feasibility of using Coherent Anti-Stokes Raman Spectroscopy (CARS) to study the pheonomenon of muzzle flash is assessed. The experiment reported here consisted of firing a modified M-14 rifle into a large metal box purged with nitrogen while probing the resulting flow field with spark shadowgraphs, a He-Ne laser and colinear laser beams used for CARS signal generation from carbon monoxide. Results of the light transmission experiments indicate the times and positions in the muzzle flow field where CARS may be used to obtain

DD FORM 1 JAN 73 1473 EDITION OF 1 NOV 65 IS OBSOLETE

UNCLASSIFIED

SECURITY CLASSIFICATION OF THIS PAGE (When Data Entered)

20. Abstract (Cont'd):

temperature measurements. Both narrow-band and broad band CO CARS signals were generated at an axial location 7.5 cm downstream of the barrel exit at times of 1.0, 2.0, and 3.0 milliseconds after bullet exit. These signals appear sufficiently large for determining spatially and temporally resolved temperatures. The direction of future muzzle flash temperature studies is also given.

TABLE OF CONTENTS

FIGURE CAPTIONS

I. INTRODUCTION

Muzzle flash is observed during the operation of large and small caliber guns. It typically appears as a bright flash of light outside the muzzle and is associated with the release of rich combustion products from the barrel of the gun. Controlling and suppressing this phenomenon is of major practical concern since the energy release is sufficient to produce blast waves and large visible/thermal signatures, both being of use in locating the position of the gun.

Past studies[1-3] have indicated the existence of three separate regions of flash. They are, in order of increasing distance from the muzzle: primary, intermediate, and secondary. Luminosity from these three regions arises primarily from glowing particulate and sodium emission. Thus, the spectrum associated with muzzle flash displays line emission, as well as a broad background emission characteristic of blackbody radiation. Primary flash occurs at the barrel exit and is a result of the hot, luminous combustion products leaving the muzzle after the bullet uncorks. Subsequent rapid expansion of the combustion gases quenches much of the remaining gas phase reaction, thus producing a dark region following the primary flash. As the process continues, over-expansion leads to the formation of a Mach disk (normal shock wave) downstream of the muzzle. This shock structure reheats the incomplete combustion products and initiates new combustion. As a result, a second luminous region develops downstream of the Mach disk and is called the intermediate flash whose major products contain CO and H_2. By this time, the growing flow field begins to entrain air and a third combustion region develops (the secondary flash). Combustion of CO, H_2, and other fuels with air here accounts for a major portion of energy release occurring outside the gun barrel.[4]

The study of muzzle flash is motivated by the desire to control and suppress the secondary flash. It has been observed that small amounts (1-2%) of an alkali metal salt added to the propellant will often suppress the flash, but the mechanisms associated with the suppression are not well understood. For example, it is still unclear whether these metal salts act thermally or chemically, and if the latter, whether the process occurs heterogeneously (i.e., on the surface of a particle) or homogeneously in the gas phase. Recent studies[5,6] has shed some light on this subject, but much work remains to be done.

When muzzle flash is considered in the context of studying the condition leading to its suppression, the relevant mechanisms involved must often be guessed at. The reason for this is a lack of information on the conditions present within the developing muzzle flow field. High luminosity, extreme density gradients, high concentrations of particulates, and the transient nature of the event are all responsible for preventing many of the traditionally accepted diagnostic techniques from being applied. Williams and Powell[7] and Lederman, et al.,[8] have both used laser Raman spectroscopy to investigate the muzzle blast region of a 20 mm gun. Both studies used down-loaded rounds which achieved muzzle velocities in the neighborhood of 400 m/s. Williams and Powell looked at the region from 0.32 and 1.3 cm downstream of the barrel exit for times up to 3 milliseconds after the projectile exit. Laser induced particulate incandescence prevented direct measurements of temperature, but relative densities for N_2 and CO were obtained. These

relative values, however, were based on an assumed gas temperature, and thus, the results of Williams and Powell can at best be qualitative. Lederman, et al., observed a position of 5 cm downstream of the muzzle exit for a time frame of 0.33 to 2 milliseconds. Over this region they obtained an essentially constant temperature of ~1500 K. The lack of a time dependence on temperature caused the authors to question the measurements, but they could not substantiate alternate explanations. Petrow and Harris[9] have looked at the muzzle flash of a 7.62 mm gun using CARS. They searched for the CARS signal of the H_2 molecule in the muzzle flash region. Due to nonsynchronous triggering of the laser with respect to the gun firing, only one H_2 spectrum, with a low signal-to-noise ratio, was obtained in several hundred shots. Klingenberg and Mach used a non-laser diagnostic technique based on sodium and potassium line reversal to obtain temperature measurements of the intermediate and secondary flash regions. Such a technique is generally applicable where the probe region is luminous and where the Abel-inversion technique for data analysis is valid, i.e., an axisymmetric temperature distribution and a uniform alkali metal concentration.

Although the CARS approach is more sophisticated than line reversal techniques, it appears to be well suited for obtaining temperature and concentration profiles in the muzzle flash region. It is non-intrusive and capable of a high degree of spatial and temporal resolution. In addition, the CARS signal emerges as a collimated beam making it ideal for minimizing interference associated with incandescence and luminosity from the probe volume. This method relies on the ability of high energy lasers to pass through the flow field, hence, its applicability is limited to systems of relatively high light transmission.

Typical solid propellants burn rich giving the major products of combustion as approximately 40% CO, 17% H_2, 16% H_2O, 14% CO_2, and 11% N_2.[10] In the work reported here, CO has been chosen as the target molecule for the CARS technique. There are several obvious reasons for this choice. Diatomic spectroscopy is simpler than triatomic, thus eliminating H_2O and CO_2 as possible candidates. N_2 is present in air, which can lead to problems when using the colinear geometry for generating CARS signals. CO and H_2 still remain as candidates; however, CO is present in larger concentrations and there exists more efficient dyes for producing the Stokes beam appropriate for CO than for H_2. One further point should be made with reference to the H_2 molecule. Since H_2 has such a large rotational constant, the individual rotational lines within the v_{0-1} Q-branch of H_2 are well resolved. This permits a simpler computation, as well as permitting lower temperatures to be determined more precisely. This well resolved structure has a drawback which arises when taking single shot data. The shot-to-shot fluctuations of the dye laser can introduce serious errors into the data analysis unless the laser frequency envelope (amplitude as a function of frequency) is monitored with each laser pulse. This monitoring adds to the experimental complexity, and consequently, CO is deemed the choice molecule.

In this paper, we present data on the feasibility of using the CARS approach to study the muzzle flash phenomenon. Spark shadowgraphs and light transmission data for various locations in the flow field are presented. Also, broadband CARS signals are presented demonstrating the acquisiton of signals that can later be used for obtaining temperature measurements.

II. EXPERIMENTAL DESCRIPTION

The experimental apparatus consisted of a modified M-14 rifle having a nominal muzzle diameter of 7.62 mm and a shortened barrel length of 451.5 mm. This previously used barrel length has been incorporated here so that a comparison with past studies[2 11 12] can be made. The rifle was held in a framework which was attached to a large metal box of dimensions 0.6 x 1.0 x 1.4 meters. Design features of this box included a retractable flat flame burner for generating rich CO/O_2 flames, a vent for gas removal, and a nitrogen line for purging. In addition, Plexiglas windows were incorporated into the design to provide optical access to the interior regions of the box. However, for CARS signal generation, simple free air access ports were provided through the Plexiglas because of the high power of the laser pulses. For trapping the bullets during each experiment, a bullet catcher was used on the opposite side of the box from the rifle.

Standard ball ammunition with WC-846 deterred surface coated propellant has been used for all data reported here. Table 1 lists the chemical composition of this propellant. It is made up of nitroglycerin and nitrocellulose with small amounts of calcium carbonate and sodium sulfate. The nominal mass of propellant in each round was 2.99 gm. When used in the barrel with dimensions specified above, this gave a muzzle velocity of approximately 840 meters/second.

Table 1. Composition of WC-846 Propellant

Component	% (By Mass)
Nitroglycerin	9.71
Dinitrotoluene	0.71
Diphenylamine	0.90
Nitrocellulose	87.01
Calcium Carbonate	0.46
Sodium Sulfate	0.07
Moisture and Volatiles	0.85
Residue Solvent	0.29

Our studies began by measuring the light emission, primarily secondary flash, with a photodiode when firing into air. Figure 1 displays the temporal profiles of the light observed 18 cm downstream of the muzzle exit for four shots. These dual oscilloscope traces were triggered by the breaking of a He-Ne laser beam positioned at the muzzle exit. The bottom trace represents the detected He-Ne laser light where the high value indicates total blockage of the beam and the low value full transmission. The top traces are the muzzle flash light emission. Light emission begins about 1.2 milliseconds after bullet exit and lasts for about 1 millisecond. However, as can readily be observed, there is substantial shot-to-shot variation. This variation is indicative of the stochastic nature of secondary flash due to the turbulent mixing of air with the combustion products coming from the gun barrel. Such a situation is unacceptable for a single shot CARS experiment because of the irreproducibility of the process. To properly access the data in such a situation, it would be necessary to build a probability distribution function

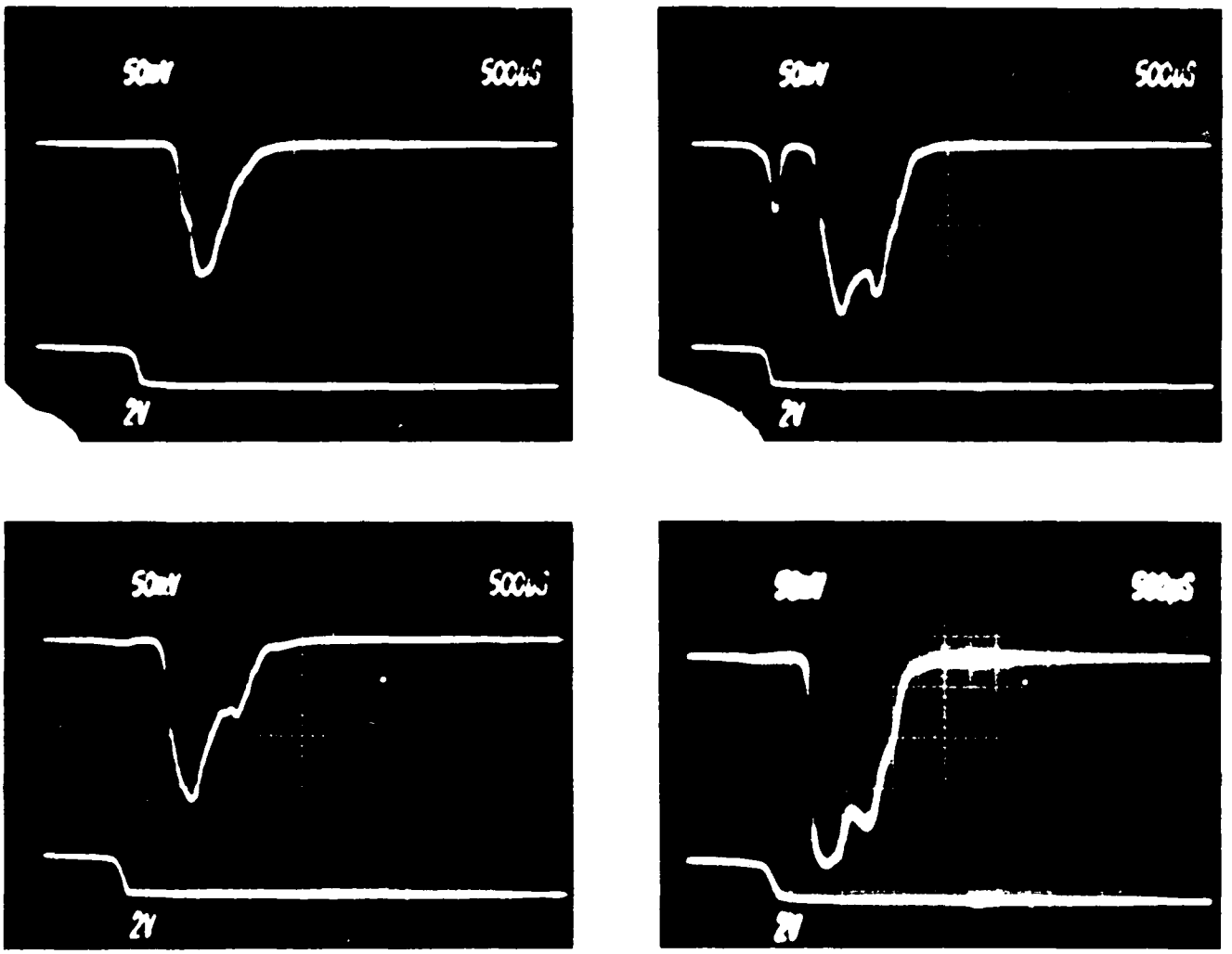

Figure 1. Light Emission from the Muzzle Flash of a 7.62 mm Rifle Using Standard Ball Ammunition. Measurement point 18 cm downstream of muzzle exit. Horizontal time scale is 500 microseconds. Vertical scale is light intensity in arbitrary units. All four shots repeated under identical conditions.

for the secondary flash region which would be extremely time consuming. Since the intermediate flash is less turbulent than the secondary flash, and since the present ideas[12] suggest that it is the controlling region for generating secondary flash, we decided to perform the measurements here. Purging the box with nitrogen suppressed the secondary flash, thus eliminating most of the light emission and blast effects from the experiment. Still present, however, were the primary and intermediate flashes and the gas dynamic processes associated with them. An example of the primary and intermediate flash is shown in Figure 2, where the small amount of light at the muzzle exit is the primary flash. The photograph was taken under self-light conditions as the gun fired into a nitrogen atmosphere.

Figure 2. Self-Light Photograph of Primary and Intermediate Flash

For a qualitative picture of the developing muzzle flow field, we employed the technique of spark-shadowgraph photography similar to that used previously.[14] A short duration (<5 microsecond) point light source was placed approximately 2.5 meters from the gun-box setup. The optical path was through a pair of openings in opposite sides of the box. A large Fresnel lens collected light passing through the viewing region and a simple open shutter

camera, with a blue gelatin filter, recorded the resulting image. This filter permitted the transmission of light from the short duration spark source while blocking the sodium emission from the primary and intermediate flash regions. Film speed used in the camera was ASA 1200. A variable delay for the spark light source, triggered by the interruption of a He-Ne laser beam positioned at the exit of the gun barrel, provided a means of obtaining photographic records for different times in the experiment. Semi-quantitative data on the light transmission through the flow field were provided by a series of simple experiments employing a He-Ne laser and a photodiode detector, as shown in Figure 3. The laser was directed through the flow field at specified downstream locations from the barrel exit. Laser path and barrel axis were perpendicular. During the experiment a storage oscilloscope recorded the detector response. An effort was made to ensure that the detector behaved in a linear fashion to the amount of light received. Effects of beam steerage were explored by performing experiments with both a large detector surface, and one where only a small aperture in front of the detector surface was used. No apparent differences were present between the two sets of data.

CARS spectra for CO were obtained during gun firing using the experimental setup shown in Figure 4. This arrangement, along with the triggering system described later, provided the opportunity for recording single shot CARS signals during the experiment. A colinear phase matching scheme was employed with pump beam and Stokes beam wavelengths of 532 nm and 600 nm, respectively. The latter value was the center of the broadband dye laser emission (in zero order) which had a band width of approximately 4 nm. This permitted data to be obtained from ground and vibrationally excited levels of the CO molecule, thus yielding vibrational temperature information on the molecules in the probe volume. A previous study[15] on CO in a diffusion flame used a binary dye mixture of Rhodamine 640 (R-640) and Kiton Red (KR) for the dye laser. Our choice of dyes was similar with approximate percentages by weight of 70% R-640 and 30% KR. Exact dye mixture concentrations were adjusted during laser operation to "peak" the output while observing CARS signals of hot CO from a burner. This proved to be the most expedient manner in which to obtain the correct broadband emission output.

The optical train consisted of a Quantel, Model YG-481C, Nd:YAG laser with frequency doubling, a Quanta-Ray, Model PDL-1, pulsed dye laser, and various anti-reflection coated optics to direct and combine the vertically polarized CARS signal-generating laser beams as shown in Figure 4. The 532 nm radiation was separated from the 1064 nm residue, left over from doubling, by a dichroic mirror. Frequency doubled output from the Quantel unit was measured as approximately 300 millijoules per pulse. Of this, a beam splitter directed 60% to pump the dye laser which produced a Stokes beam energy in the range of 30 to 40 millijoules per pulse. The remaining 40% was directed to a beam expander. Path lengths of both the Stokes beam and the pump beam were matched and then the two beams combined into one with the use of a dichroic mixer with 75% efficiency. To improve the spatial resolution of this colinear geometry, the pump beam was expanded to 2.06 cm. Next, a pair of anti-reflection coated 30.5 cm focal length lenses were employed to direct the CARS generating beams into the probe voluem and then to recollimate the emerging radiation which included the CARS signal.

Also shown in Figure 4 are the details of the CARS signals acquisition system. After the collecting lens recollimated the emerging laser beams and

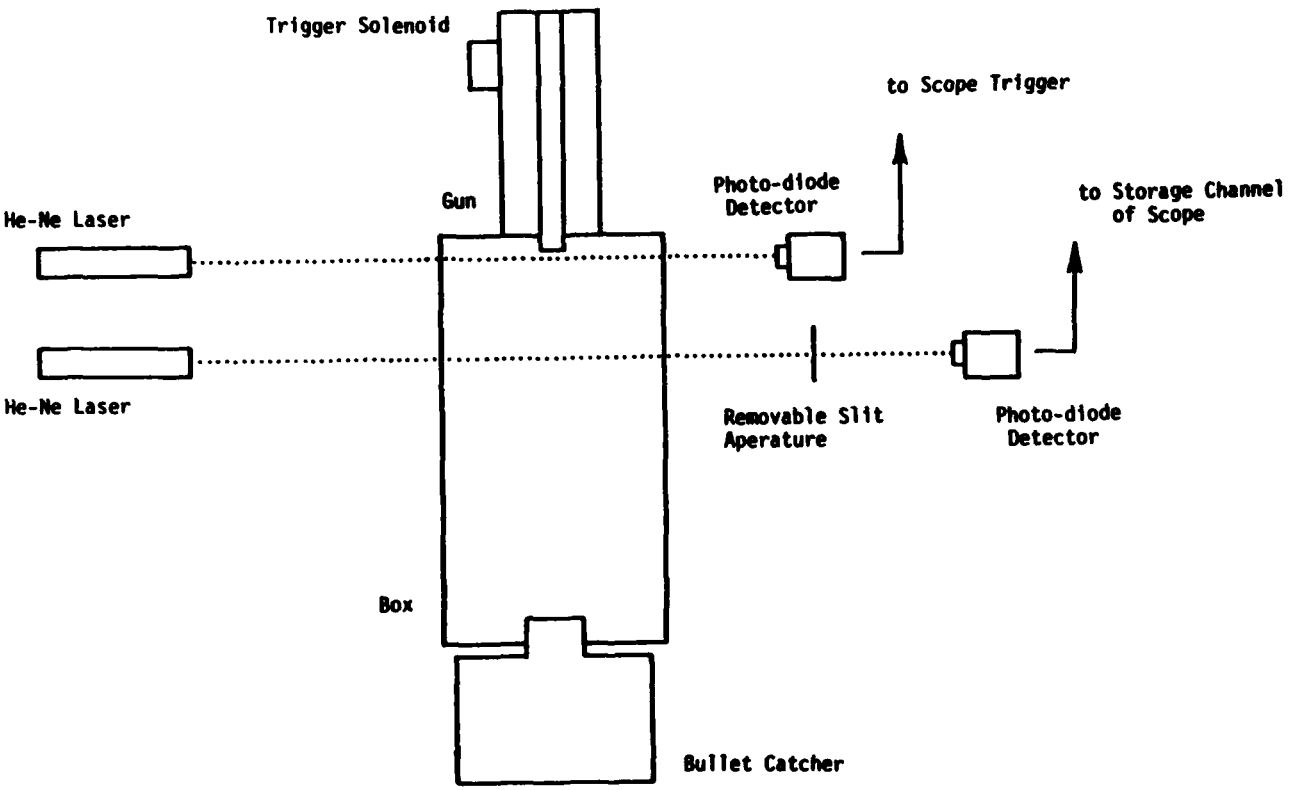

Figure 3. Schematic Diagram of He-Ne Laser Transmission Setup

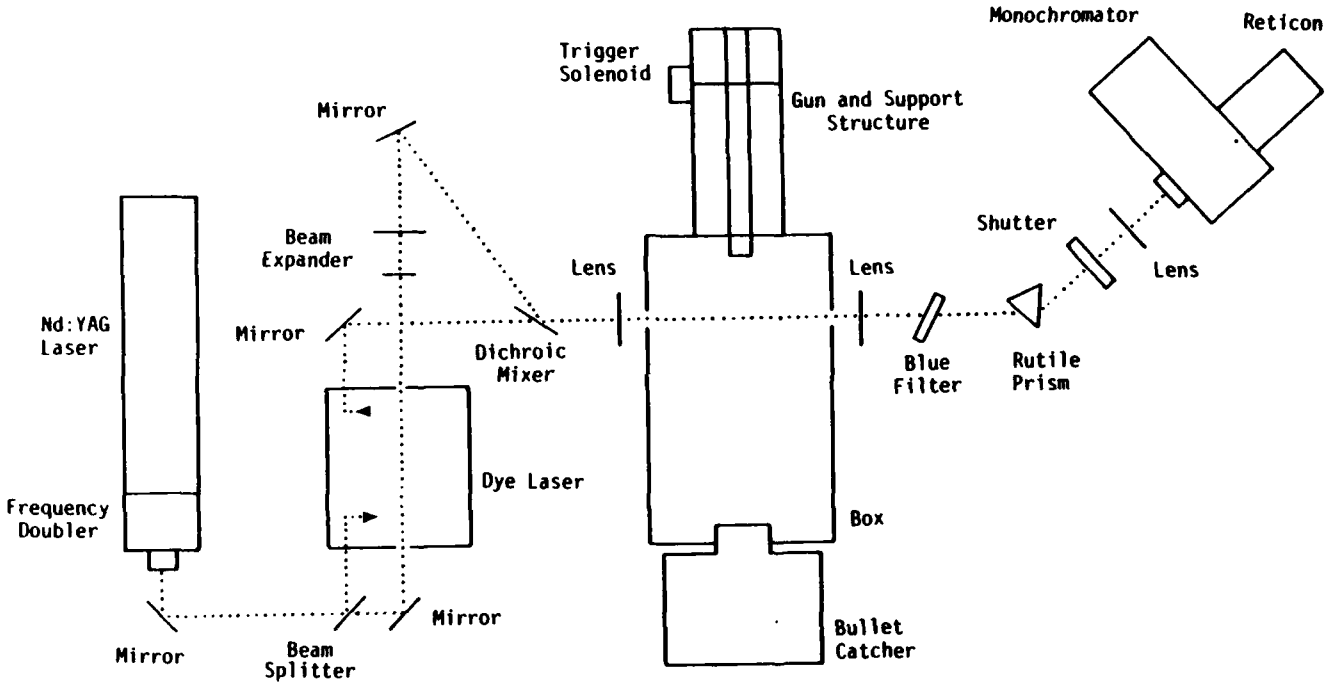

Figure 4. Schematic Diagram of Experimental Arrangement Used to Record CARS Signals

CARS signal, a blue filter was used to reject most of the 532 nm and 600 nm radiation from the signal train leaving the CARS signal at 478 nm. Further separation was achieved by the rutile prism which directed the light toward a focusing lens. By the time the light reached the 300 micrometer wide entrance slit of the quarter meter monochromator, the CARS beam was sufficiently isolated so that only it passed into the monochromator. A 2400 groove/mm grating was used to disperse the signal and a microchannel image intensifier with an optical multichannel reticon detector recorded the resulting CARS signal.

The FWHM resolution of the detection system, determined from Na-D lines, was approximately 14 cm^{-1}. The sampling volume approximated a cylinder of 0.01 cm in diameter which had a length that was experimentally determined by translating a 1 mm thick glass slide through the CARS interaction zone while monitoring the non-resonant signal. A plot of the peak height of the CARS signal vs. position is shown in Figure 5. Spatial resolution is commonly defined as the position at which the signal drops to 1/e of its maximum value, and using this criterion, the interaction cylinder length was determined from Figure 5 to be 0.55 cm.

Although the details of the timing circuitry will be presented in the next section, the operation of the detection system requires some explanation here. The gun firing mechanism consisted of a solenoid actuated trigger. From the time the solenoid is energized to the time the bullet exits the barrel, approximately 20 milliseconds elapsed. At the same time the trigger sequence is begun, the control unit of the OMA receives a signal initiating a time interval of 200 milliseconds during which the detection elements of the reticon are active. Also during this time interval, a shutter is opened for approximately 100 milliseconds. In this way, detection of CARS spectra originating from a single laser pulse was achieved.

III. EXPERIMENTAL TIMING

There were two major design constraints in developing the laser control circuitry. The first was associated with the need to have the laser pulsing continuously (at 8.9 Hz*) while adjusting the system for maximum signal generation. The second constraint involved synchronizing a single laser pulse with the firing of the gun for acquiring data. This latter constraint meant precisely triggering the laser (within a few microseconds) from a repeatable source. We chose the interruption of a He-Ne laser beam positioned in front of the gun barrel as the trigger source of the laser.

A schematic diagram of the timing system is shown in Figure 6. The hardware used to fulfill the experimental requirements proved to be an integration of a specially built, one-shot control circuit with the commercial

---

*Normally the laser operates at 10 Hz, however, due to the aging of the power supply, it now takes longer to charge the capacitor bank when operating at full power. This required a reduction in the repitition rate to ensure adequate time for charging.

laser control unit. During pre-firing optical adjustments, the laser ran at a set internal frequency of 8.9 Hz. However, when a single laser pulse was to be synchronized with the gun firing, the one-shot circuit assumed control of the experiment. The following sequence of events describes the operation of the system.

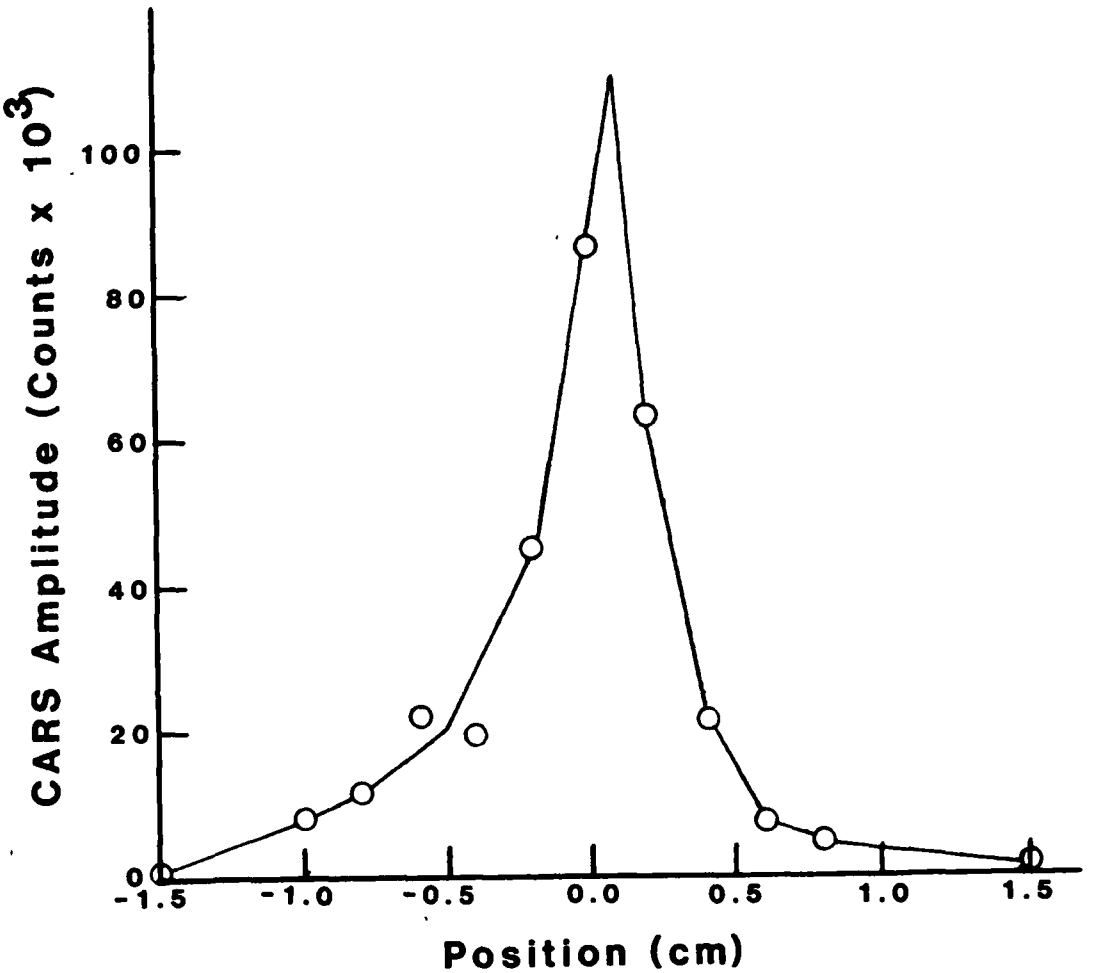

Figure 5. Spatial Resolution of Probe Volume as Given by a Plot of the CARS Signal Intensity Generated from a Glass Slide Vs. Position Across Probe Volume

CARS signal generation was first optimized with the laser pulsing at 8.9 Hz. At the time the experiment was to start, the operator actuated a push button (master start) which signaled the one-shot circuit to assume control of the experiment on receipt of the next laser charge order. Upon receiving the order, the micro-relay (see Figure 6) was de-energized, thus inhibiting the laser from firing on its own. The reason for this is that when the micro-relay is closed, the rotary switch of the laser control unit was grounded, thus allowing the end-of-charge order to trigger the laser. When the relay was open, the switch floated high preventing the end-of-charge from being acted upon. However, when this order was issued by the laser control

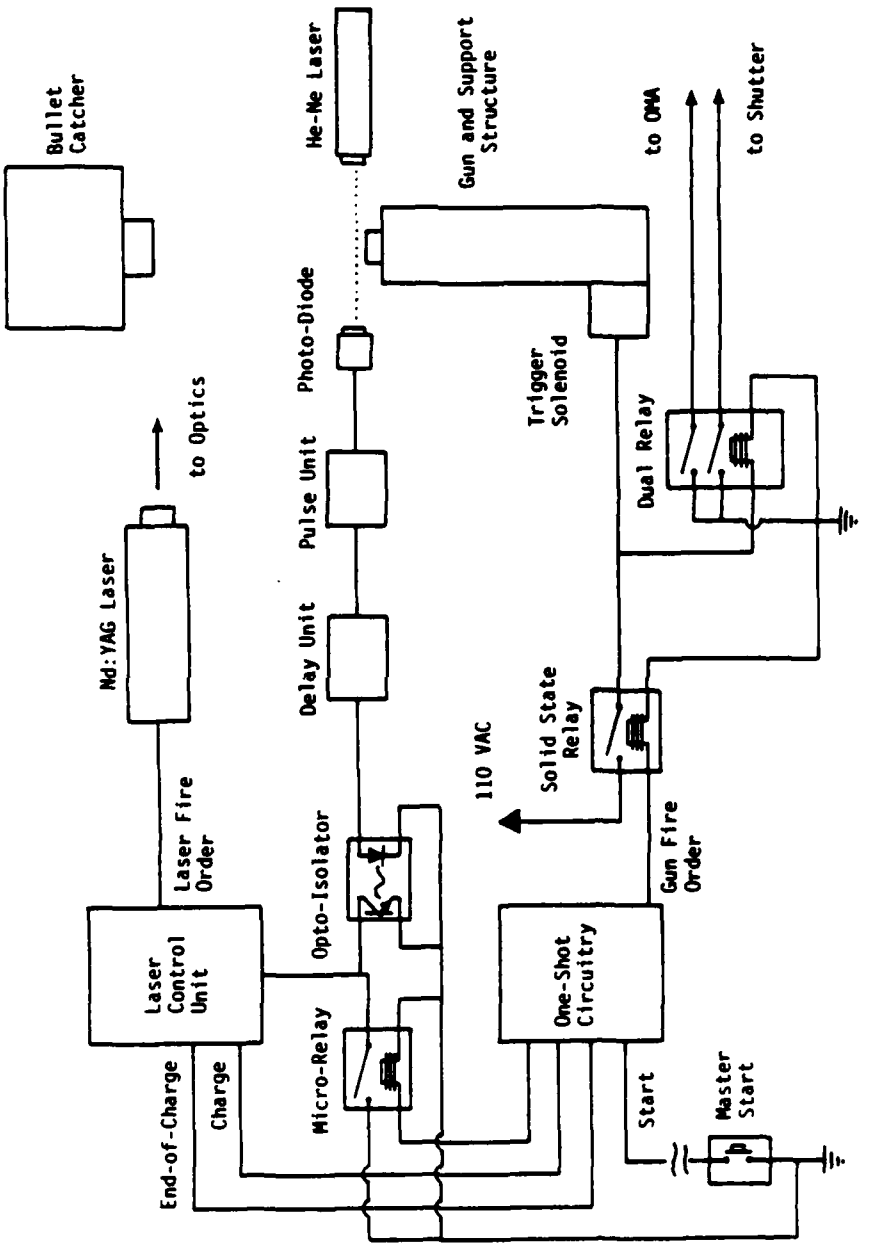

Figure 6. Schematic Diagram of Trigger and Timing Setup

unit, the one-shot circuit issued a gun firing order by energizing the solid state relay, triggering the OMA, and opening the shutter. Approximately 20 milliseconds later, the bullet emerged from the barrel interrupting the He-Ne laser beam. The resulting output pulse from the photo-detector, through an appropriate delay, triggered the laser by bringing the rotary switch on the laser control unit to near ground potential through the optical isolator. It should be noted that the logic for the one-shot circuit was built from CMOS chips operating on a 15 volt power supply. This choice was dictated by the requirements of extremely high noise immunity and compatibility with the logic of the laser control unit.

We should point out that the procedure described above triggers the flash lamps of the Nd:YAG laser. The actual lasing process occurs 200 microseconds later when the laser oscillator is Q-switched. Thus, if data at times less than 200 microseconds were required, a modified triggering procedure would be needed. The data reported here have been independently timed by monitoring a portion of the 532 nm radiation reflected from the blue glass filter. Thus, the data recorded at 1, 2, and 3 milliseconds reflects the true time interval between the interruption of the He-Ne laser and the detected CARS signal. Jitter associated with these times could not be assessed at the delays (<1 millisecond) used in these experiments because of the limited resolution of the oscilloscope used to record the timing pulses. We believe, however, that an upper limit of approximately 10 microseconds is the associated overall jitter that exists for the timing system used.

The characteristic times of the experiment include those associated with the data acquisition system and the muzzle flow field. The laser system operated at a free running time-between-pulses of 115 milliseconds (8.9 Hz). From the time at which the trigger solenoid was energized to the time at which a bullet emerged from the barrel, approximately 20 milliseconds elapsed. The muzzle flow field developed on time scales of the order of 5 milliseconds while primary and intermediate flashes occurred in the first millisecond after the bullet leaves the barrel. Through the use of the variable delay unit that transmitted the laser fire order to the opto-isolator, the data acquisition time could be varied from near zero (time bullet uncorks) to beyond 10 milliseconds. Thus the laser timing allowed virtually all times of interest in the developing muzzle flow field to be studied.

IV. RESULTS AND DISCUSSION

Figure 7 shows a sequence of five shadowgraphs obtained at various times after the bullet emerges from the barrel. The clarity of these photographs reveal important structure in the muzzle flow field as the combustion products expand into a nitrogen atmosphere. The first frame, obtained at a delay of 250 milliseconds, shows the bullet, shock wave, and the turbulent flow field. The photograph reveals the existence of a dark zone that may indicate the presence of a high, localized concentration of particulates. Later times in the event show the particulate cloud moving downstream and a shock structure forming outside the barrel. This latter effect is evidenced by the formation of a Mach disk which travels toward the barrel exit as the expansion subsides. These photographs indicate the severe environment existing when the gun is fired.

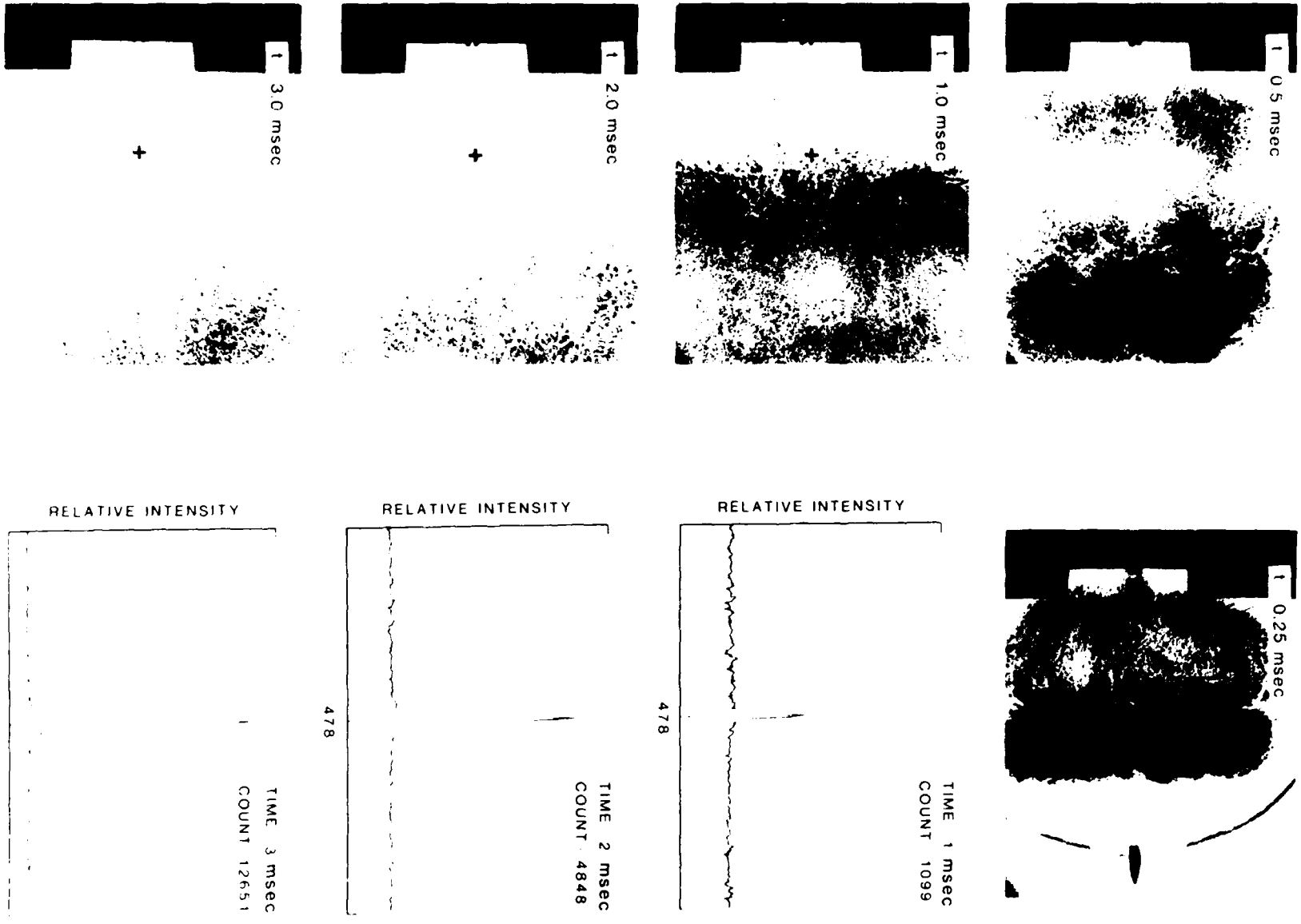

Figure 7. Sequence of 5 Shadowgraphs of the Developing Muzzle Flow Field Recorded at 0.25, 0.5, 1.0, 2.0, and 3.0 Milliseconds After Bullet Exit. Also shown are the narrow band CARS signals for CO at 1.0, 2.0, and 3.0 milliseconds. The + symbols on the shadowgraphs indicate the position where the CO CARS data is obtained.

Figure 8 shows a series of curves obtained from oscilloscope records of the photodiode response. This data represents the transmission of the He-Ne laser beam across the barrel axis for downstream locations of 5, 7.5, 10, 15, and 20 centimeters. Although shot-to-shot variations occurred, we have presented typical curves for each axial position. The baseline value in each of the curves represent the fully transmitting condition, while the maximum levels indicate total blockage of the beam. All curves show nearly total blockage at some time during the event. For example, at 7.5 cm, this blockage occurs rapidly and lasts for approximately 200 microseconds. At 15 and 20 cm, the blockage is produced first by the bullet passage, as shown by a sharp peak in the data, and then by the following particulate-laden flow. These curves indicate the existence of times during the event when data may be difficult to obtain, and other times when the flow field may be successfully probed with laser based diagnostic techniques. A frequent question arises as to how close to the muzzel exit can the flow field be optically probed. From the results of Figure 8, as well as other photodiode results (not shown), we speculate that positions from 1-5 cm downstream of the muzzle exist which can be probed at times >300 microseconds after bullet exit.

Narrow band CARS signals for CO during gun firing are presented in Figure 7. They were obtained by using a Stokes wavelength of 600.5 nm which is specific for the ground vibrational state of carbon monoxide. The data were recorded at a downstream axial position of 7.5 cm indicated by the symbol (+) in the spark photograph. The purpose of recording these narrow band signals was to compare the resonant signal strengths to the non-resonant ones. This was accomplished by first recording data at 600.5 nm, then repeating the experiment at a wavelength off-tuned from this value by 0.3 nm. Consistent results were obtained and for the 3 millisecond case, the peak resonant signal represented approximately an order of magnitude larger signal strength than the non-resonant one. This was also true for the 2 millisecond case, although the signals were less intense. Resonant signal strengths for 1 millisecond were not strong enough to make a meaningful comparison.

Broadband CARS signals, recorded near 478 nm, are shown in Figure 9. These spectra are a result of operating the Quanta-Ray dye laser in zero order and without the frequency narrowing etalon. Also, each curve represents data originating from a single laser pulse due to the transient nature of the experiment. These broadband spectra are influenced greatly by the broadband output from the dye laser. The quality of this output is presented in Figure 10. Three non-resonant background signals obtained from nitrogen in the probe volume prior to gun firing are shown. These curves are single shot results and show the broadband characteristics of the dye laser output.

A comparison of the broadband CO CARS signals from the muzzle flow field at 2 milliseconds (bottom curve) and from a rich CO/O_2 flat flame is shown in Figure 11. The two spectra were obtained at the same nominal laser operating parameters. Emission from the flame in the blue region of the spectrum is responsible for the interference observed in the recorded CARS signal. Although this interference is large, it is evident that the carbon monoxide from the burner is hot because substantial excitation of higher vibrational levels is observed. From previous experiments conducted with the burner using spontaneous Raman spectroscopy in the post flame gases, the temperature of the hot carbon monoxide was measured to be approximately 1700 K. The CARS spectrum obtaining during the gun firing at a delay of 2 milliseconds does not

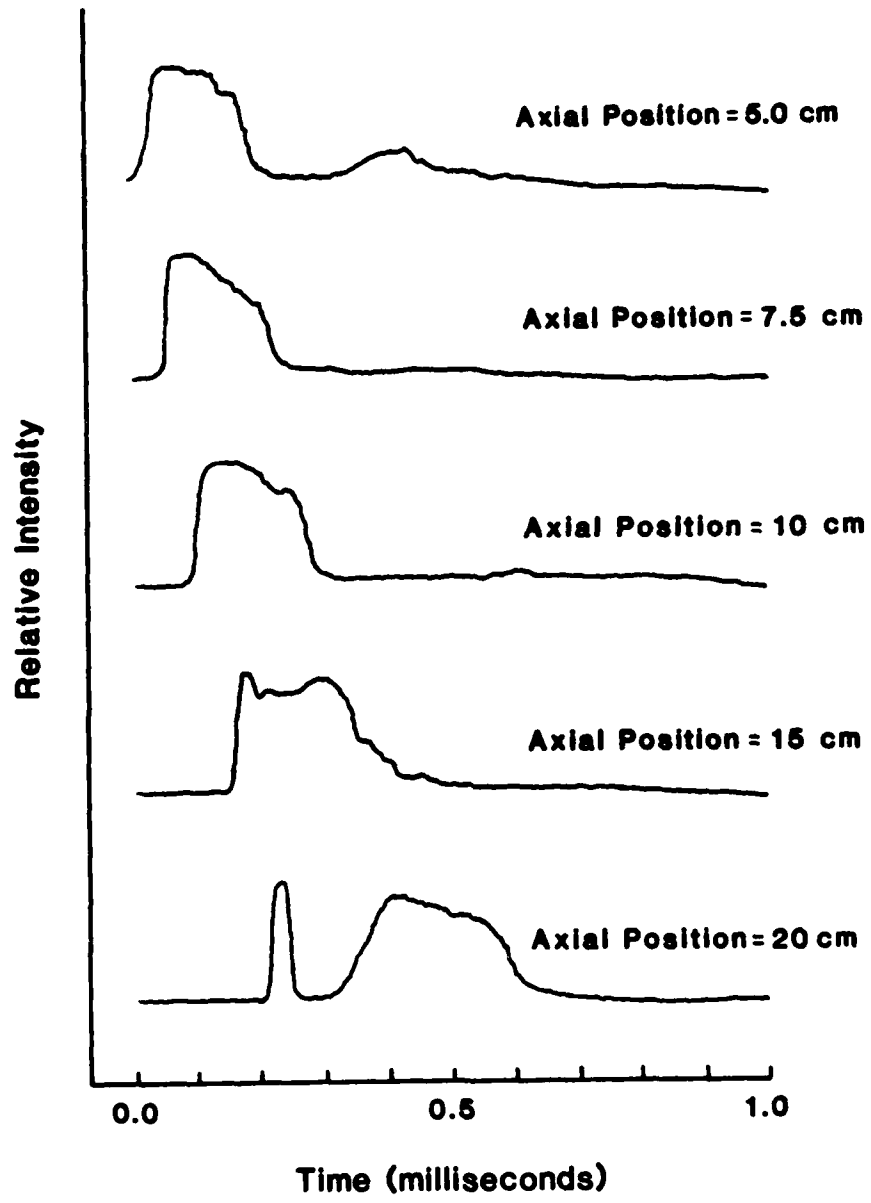

Figure 8. He-Ne Light Transmission Data for Various Locations Downstream of the Muzzle

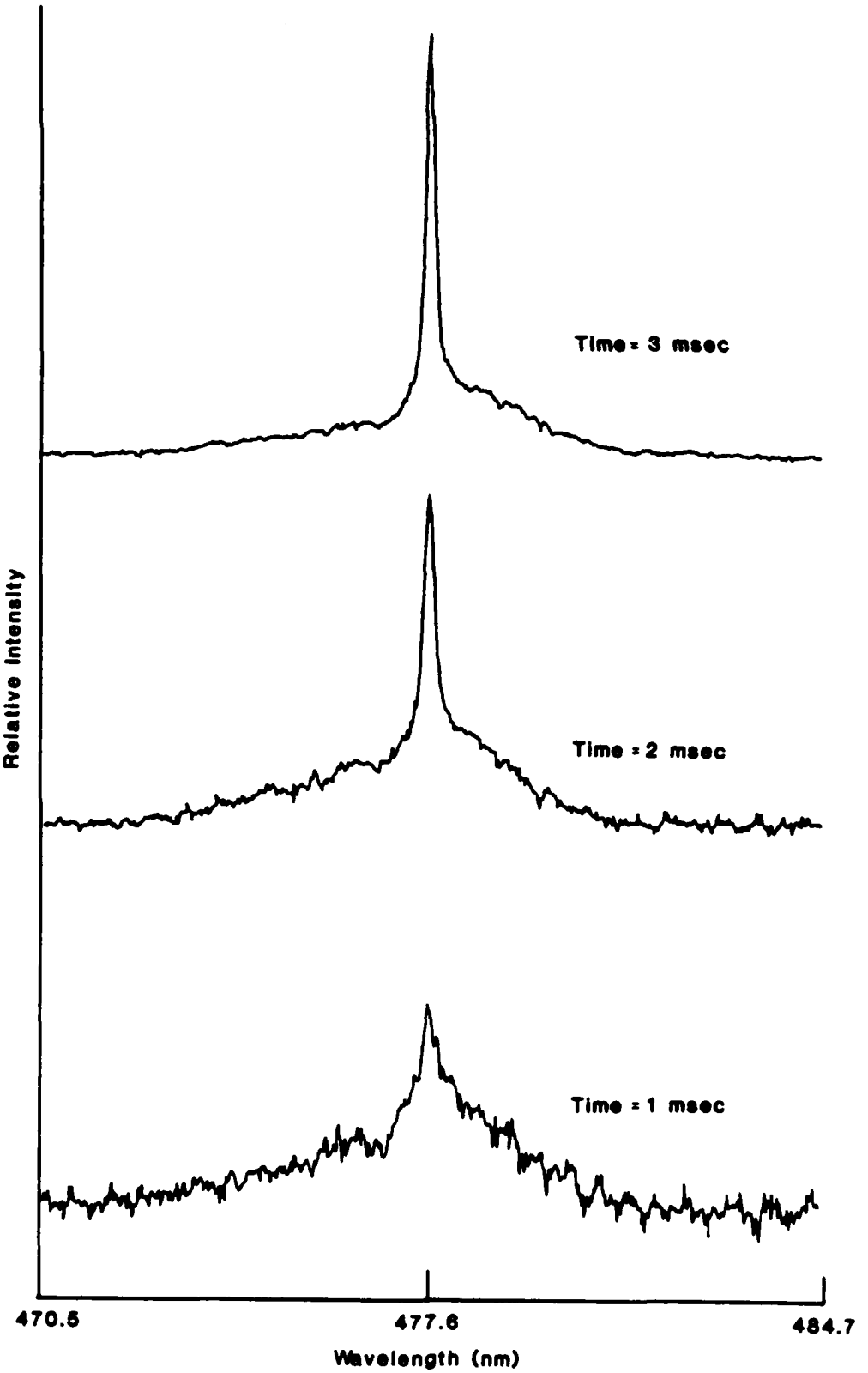

Figure 9. Broadband CARS Signals from Carbon Monoxide in the Muzzle Flow Field at Times of 1.0, 2.0, and 3.0 Milliseconds

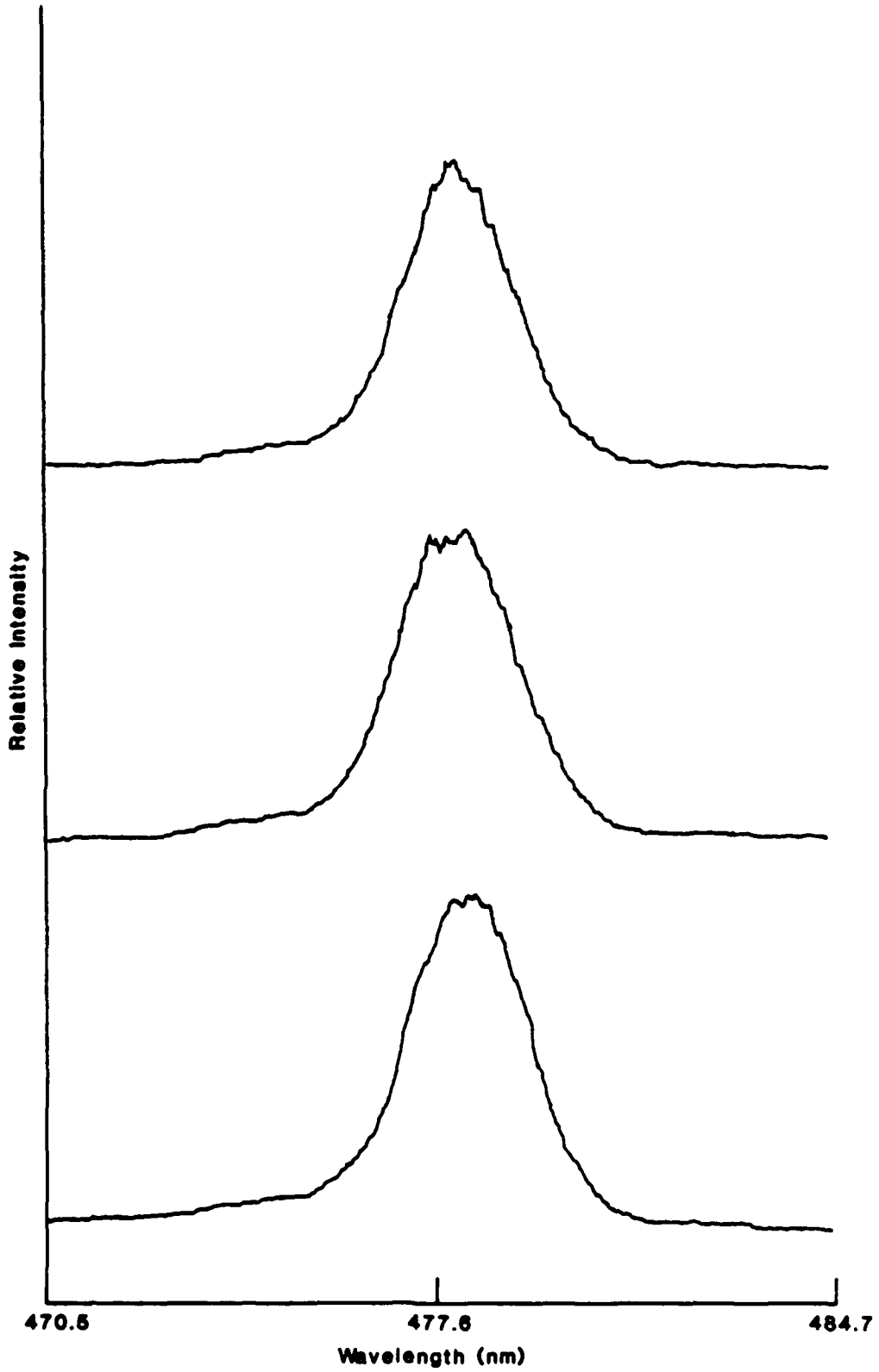

Figure 10. Non-Resonant Broadband CARS Signals from Nitrogen in the Probe Volume

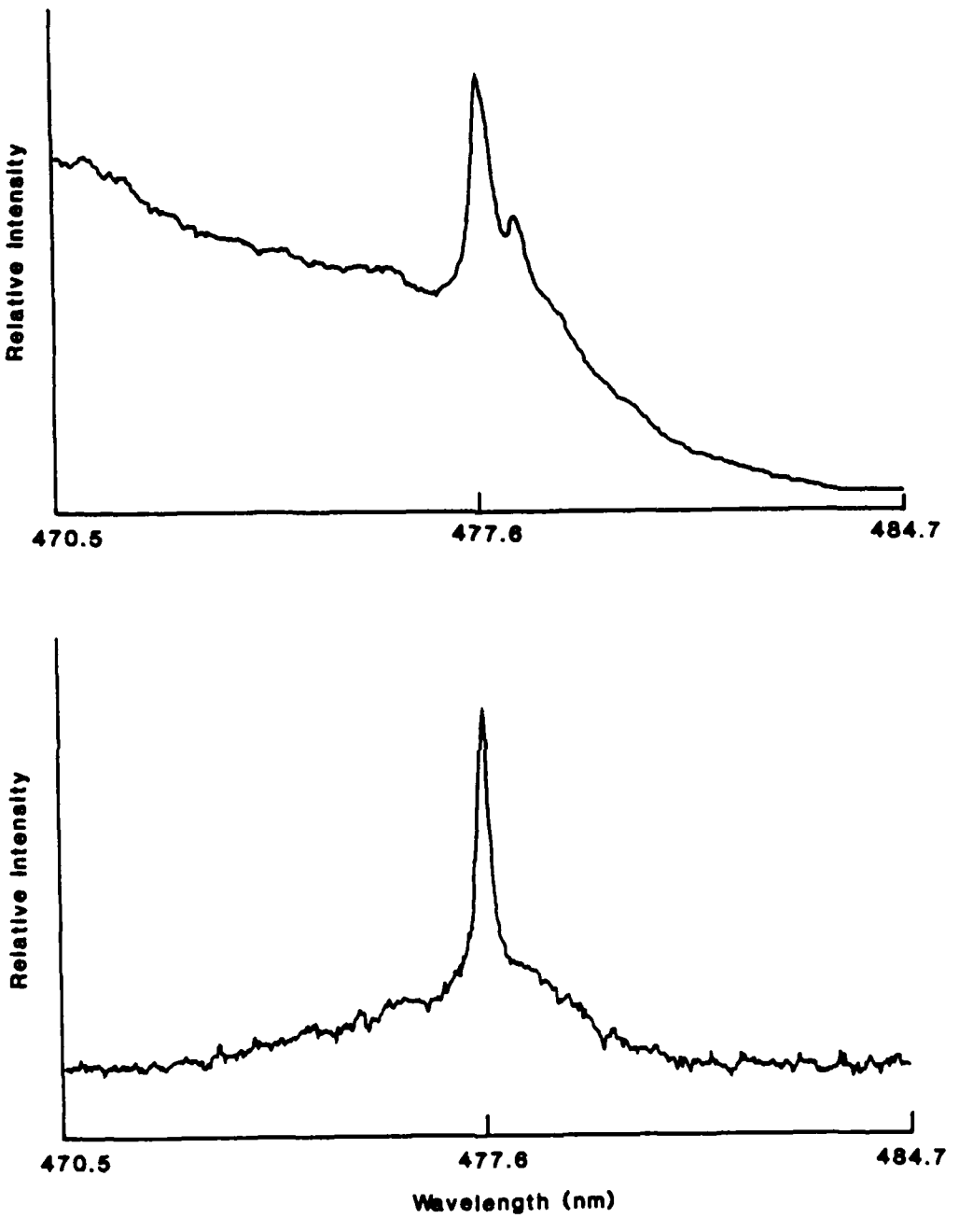

Figure 11. Comparison of CARS Signals from Muzzle Flow Field and CO/O_2 Flat Flame

display activation of the second vibrational level, and thus, indicates a much lower temperature. This is also true for data collected at 3 milliseconds.

At this point we have not completed revising the CARS fitting program appropriate for carbon monoxide; nonetheless a very crude upper limit for the temperature of the muzzle flow field can be estimated by a comparison with calculated CARS spectra[16] for N_2. The second vibrational level is only noticeably observed for temperatures greater than 1000 K which we place as the upper limit for the temperature at 7.5 cm downstream of the muzzle exit at times greater than 2 milliseconds. For the 1 millisecond case, noise associated with the recorded signal prevent any conclusion from being made. No other published temperature data have been reported for identical conditions, thus a direct comparison is not available. This 1000 K temperature is substantially below other reported intermediate flash temperatures; Klingenberg and Mach[2] measure temperatures around 1800 K, 10 cm downstream of the muzzle exit at times around 0.9 millisecond after bullet exit. Several explanations for this low upper limit are plausible. Intermediate flash lasts for about 1 millisecond, and thus, substantial cooling can take place at longer times. The position 7.5 cm downstream of the muzzle exit is on the leading edge of the luminous portion of the intermediate flash region (see Figure 2a of Reference 9), and thus, is not representative of the conditions within the intermediate flash region.

It is also believed that this 7.5 cm position is responsible for the apparent disappearance of the CARS signal at times shorter than about 1 millisecond. This situation is unfortunate, but can be explained in terms of pressure variations of the muzzle flow field. Klingenberg[11] has measured the pressure history for an identical rifle at a position 7.5 cm downstream from the muzzle exit. Rich combustion products emerging from the muzzle expand adiabatically into surroundings. During the course of this expansion, gas pressure decays from approximately 200 atmospheres to subatmospheric pressure (approximately 0.3 atm). For the position of 7.5 cm downstream from the muzzle exit, Klingenberg finds that this subatomspheric pressure lasts from 0.15 to 1.2 milliseconds after bullet exit. The gas flow decelerates after passing through the inner shock front (Mach disk) which terminates the expansion. A rapid pressure jump from 0.3 to 1.6 atmospheres occurs at t = 1.2 milliseconds corresponding to the passage of the Mach disk. At later times the pressure decays back to atmospheric pressure. With respect to the CARS measurements, the signal strength is proportional to the square of density which means that signal strengths at time <1.2 milliseconds are over an order of magnitude less than those at a later time. This large change can easily cause an apparent disappearance of the CARS signal.

V. CONCLUSION

The study of muzzle flash is a difficult task due to the presence of high luminosity, extreme density changes, and high particulate loadings. These conditions vary during the course of the event, and thus, opportunities exist at certain times to apply laser based diagnostic techniques. We have demonstrated the ability to obtain CARS signals during the firing of a gun. Although these signals were recorded for times late in the event as compared

to the flash phenomenon, improvement in the experimental technique should permit the probing of the muzzle flow field during times of the actual flashing process.

VI. FUTURE STUDIES

Further studies on muzzle flash temperature measurements will involve more in-depth studies in several areas. First the CARS fitting program developed for the nitrogen molecule[17] will be revised to be able to analyze the CARS data for carbon monoxide. Second, this program will be used to determine temperatures in an experimentally well characterized CO/O_2 laminar premixed flat flame. These CARS determined temperatures will be compared with temperatures obtained from Raman spectroscopy using the same burner under analogous experimental conditions.

Once the burner studies are completed, more CO CARS spectra of intermediate muzzle flash will be attempted. Positions further downstream of the muzzle exit at shorter times will be probed to insure that we are well within the region of intermediate flash at the appropriate times. If it is determined that low temperatures persist here (negligible excitation of CO hot bands), a change to probing the CARS spectra of the H_2 molecules will be made.

REFERENCES

1. Ladenburg, R., "Studies of the Muzzle Flash and Its Suppression," BRL Report No. 618, Aberdeen Proving Ground, MD, 1947.

2. Klingenberg, G., and Mach, H., "Investigation of Combustion Phenomena Associated with the Flow of Hot Propellant Gases. I. Spectroscopic Temperature Measurements Inside the Muzzle Flash of a Rifle," Combustion and Flame, Vol. 27, p. 163, 1976.

3. Schmidt, E.M., "Secondary Combustion in Gun Exhaust Flows," BRL Report No. ARBRL-TR-02373, Aberdeen Proving Ground, MD, 1981.

4. Engineering Design Handbook, Spectral Characteristics of Muzzle Flash, AMCP 706-255, US Army Materiel Command, June 1967.

5. Mitani, T., and Niiona, T., "Extinction Phenomenon of Premixed Flames with Alkali Metal Compounds," Combustion and Flame, Vol. 55, p. 13, 1984.

6. Heimerl, J.M., "An Advanced Flash Suppression Network Involving Alkali Salts," BRL Report No. BRL-TR-2622, Aberdeen Proving Ground, MD, 1984.

7. Williams, W.D., and Powell, H.M., "Laser Raman Measurements in the Muzzle Blast Region of a 20 mm Cannon," Arnold Engineering Development Center Report AEDC-TR-79-72, AD-A088729, August 1980.

8. Lederman, S., Cresci, R, and Posillico, T., "Diagnostics of Gun Barrel Propellants," Ballistic Research Laboratory Contract Report ARBRL-CR-00519, November 1983.

9. Petrow, E.D., and Harris, L.E., "CARS Spectra from a 7.62 mm Gun," Large Caliber Weapons Systems Laboratory, Dover, NJ, Technical Report ARLCD-TR-84003, March 1984.

10. Klingenberg, G., and Heimerl, J.M., "Investigation of Gun Muzzle Exhaust Flow and Muzzle Flash," Fraunhofer-Institut fur Kurzzeitdynamik, EMI-AFB Report 1/82, 1982.

11. Klingenberg, G., "Investigation of Combustion Phenomena Associated with the Flow of Hot Propellant Gases. III. Experimental Survey of the Formation and Decay of Muzzle Flow Fields and of Pressure Measurements," Combustion and Flame, Vol. 29, p. 289, 1977.

12. Bundy, M.L., and Schmidt, E.M., "Muzzle Exhaust Flow Through a Circular Channel," BRL Report No. ARBRL-TR-03340, Aberdeen Proving Ground, MD, March 1984.

13. Heimerl, J.M., Keller, G.E., and Klingenberg, G., "Muzzle Flash Kinetics and Modeling," Fraunhofer-Institut fur Kurzzeitdynamik, EMI-AFB Report 1/88, 1985.

14. Schmidt, E.M., and Shear, D.D., "Optical Measurements of Muzzle Blast," AIAA Journal, Vol. 13, p. 1086, 1975.

15. Eckbreth, A.C., and Hall, R.J., "CARS Concentration Sensitivity With and Without Nonresonant Background Suppression," Combustion Science and Tech., Vol. 25, p. 175, 1981.

16. Eckbreth, A.C., "CARS Investigation in Sooting and Turbulent Flames," United Technologies Research Center Report R79-954196-3, East Hartford, CT, 1979.

17. Kotlar, A.J., and Vanderhoff, J.A., "A Model for the Interpretation of CARS Experimental Profiles," Applied Spectroscopy, Vol. 36, p. 421, 1982.

DISTRIBUTION LIST

No. Of Copies	Organization
12	Administrator Defense Technical Info Center ATTN: DTIC-DDA Cameron Station Alexandria, VA 22304-6145
1	HQ DA DAMA-ART-M Washington, DC 20310
1	Commander US Army Materiel Command ATTN: AMCDRA-ST 5001 Eisenhower Avenue Alexandria, VA 22333-0001
10	Central Intelligence Agency Office of Central Reference Dissemination Branch Room GE-47 HQS Washington, DC 20505
1	Commander Armament R&D Center US Army AMCCOM ATTN: SMCAR-TSS Dover, NJ 07801
1	Commander Armament R&D Center US Army AMCCOM ATTN: SMCAR-TDC Dover, NJ 07801
1	Director Benet Weapons Laboratory Armament R&D Center US Army AMCCOM ATTN: SMCAR-LCB-TL Watervliet, NY 12189
1	Commander US Army Armament, Munitions and Chemical Command ATTN: SMCAR-ESP-L Rock Island, IL 61299
1	Commander US Army Aviation Research and Development Command ATTN: AMSAV-E 4300 Goodfellow Blvd. St. Louis, MO 63120
1	Director US Army Air Mobility Research and Development Laboratory Ames Research Center Moffett Field, CA 94035
4	Commander US Army Research Office ATTN: R. Ghirardelli D. Mann R. Singleton R. Shaw P.O. Box 12211 Research Triangle Park, NC 27709-2211
1	Commander US Army Communications - Electronics Command ATTN: AMSEL-ED Fort Monmouth, NJ 07703
1	Commander ERADCOM Technical Library ATTN: DELSD-L, Reports Section Fort Monmouth, NJ 07703-5301
2	Commander Armament R&D Center US Army AMCCOM ATTN: SMCAR-LCA-G, D.S. Downs J.A. Lannon Dover, NJ 07801
1	Commander Armament R&D Center US Army AMCCOM ATTN: SMCAR-LC-G, L. Harris Dover, NJ 07801

DISTRIBUTION LIST

No. Of Copies	Organization
1	Commander Armament R&D Center US Army AMCCOM ATTN: SMCAR-SCA-T, L. Stiefel Dover, NJ 07801
1	Commander US Army Missile Command Research, Development and Engineering Center ATTN: AMSMI-RD Redstone Arsenal, AL 35898
1	Commander US Army Missile and Space Intelligence Center ATTN: AMSMI-YDL Redstone Arsenal, AL 35898-5000
2	Commander US Army Missile Command ATTN: AMSMI-RK, D.J. Ifshin W. Wharton Redstone Arsenal, AL 35898
1	Commander US Army Missile Command ATTN: AMSMI-RKA, A.R. Maykut Redstone Arsenal, AL 35898-5249
1	Commander US Army Tank Automotive Command ATTN: AMSTA-TSL Warren, MI 48397-5000
1	Director US Army TRADOC Systems Analysis Activity ATTN: ATAA-SL White Sands Missile Range, NM 88002
1	Commandant US Army Infantry School ATTN: ATSH-CD-CSO-OR Fort Benning, GA 31905
1	Commander US Army Development and Employment Agency ATTN: MODE-TED-SAB Fort Lewis, WA 98433
1	Office of Naval Research Department of the Navy ATTN: R.S. Miller, Code 432 800 N. Quincy Street Arlington, VA 22217
1	Commander Naval Air Systems Command ATTN: J. Ramnarace, AIR-54111C Washington, DC 20360
2	Commander Naval Ordnance Station ATTN: C. Irish P.L. Stang, Code 515 Indian Head, MD 20640
1	Commander Naval Surface Weapons Center ATTN: J.L. East, Jr., G-23 Dahlgren, VA 22448-5000
2	Commander Naval Surface Weapons Center ATTN: R. Bernecker, R-13 G.B. Wilmot, R-16 Silver Spring, MD 20902-5000
1	Commander Naval Weapons Center ATTN: R.L. Derr, Code 389 China Lake, CA 93555
2	Commander Naval Weapons Center ATTN: Code 3891, T. Boggs K.J. Graham China Lake, CA 93555

DISTRIBUTION LIST

No. Of Copies	Organization
5	Commander Naval Research Laboratory ATTN: L. Harvey J. McDonald E. Oran J. Shnur R.J. Doyle, Code 6110 Washington, DC 20375
1	Commanding Officer Naval Underwater Systems Center Weapons Dept. ATTN: R.S. Lazar/Code 36301 Newport, RI 02840
1	Superintendent Naval Postgraduate School Dept. of Aeronautics ATTN: D.W. Netzer Monterey, CA 93940
4	AFRPL/DY, Stop 24 ATTN: R. Corley R. Geisler J. Levine D. Weaver Edwards AFB, CA 93523-5000
1	AFRPL/MKPB, Stop 24 ATTN: B. Goshgarian Edwards AFB, CA 93523-5000
2	AFOSR ATTN: L.H. Caveny J.M. Tishkoff Bolling Air Force Base Washington, DC 20332
1	AFWL/SUL Kirtland AFB, NM 87117
1	Air Force Armament Laboratory ATTN: AFATL/DLODL Eglin AFB, FL 32542-5000

No. Of Copies	Organization
1	NASA Langley Research Center Langley Station ATTN: G.B. Northam/MS 168 Hampton, VA 23365
4	National Bureau of Standards ATTN: J. Hastie M. Jacox T. Kashiwagi H. Semerjian US Department of Commerce Washington, DC 20234
1	Aerojet Solid Propulsion Co. ATTN: P. Micheli Sacramento, CA 95813
1	Applied Combustion Technology, Inc. ATTN: A.M. Varney P.O. Box 17885 Orlando, FL 32860
2	Applied Mechanics Reviews The American Society of Mechanical Engineers ATTN: R.E. White A.B. Wenzel 345 E. 47th Street New York, NY 10017
1	Atlantic Research Corp. ATTN: M.K. King 5390 Cherokee Avenue Alexandria, VA 22314
1	Atlantic Research Corp. ATTN: R.H.W. Waesche 7511 Wellington Road Gainesville, VA 22065
1	AVCO Everett Rsch. Lab. Div. ATTN: D. Stickler 2385 Revere Beach Parkway Everett, MA 02149

DISTRIBUTION LIST

No. Of Copies	Organization
1	Battelle Memorial Institute Tactical Technology Center ATTN: J. Huggins 505 King Avenue Columbus, OH 43201
1	Cohen Professional Services ATTN: N.S. Cohen 141 Channing Street Redlands, CA 92373
2	Exxon Research & Eng. Co. Government Research Lab ATTN: A. Dean M. Chou P.O. Box 48 Linden, NJ 07036
1	Ford Aerospace and Communications Corp. DIVAD Division Div. Hq., Irvine ATTN: D. Williams Main Street & Ford Road Newport Beach, CA 92663
1	General Applied Science Laboratories, Inc. ATTN: J.I. Erdos 425 Merrick Avenue Westbury, NY 11590
1	General Electric Armament & Electrical Systems ATTN: M.J. Bulman Lakeside Avenue Burlington, VT 05401
1	General Electric Company 2352 Jade Lane Schenectady, NY 12309
1	General Electric Ordnance Systems ATTN: J. Mandzy 100 Plastics Avenue Pittsfield, MA 01203
1	General Motors Rsch Labs Physics Department ATTN: R. Teets Warren, MI 48090
2	Hercules, Inc. Allegany Ballistics Lab. ATTN: R.R. Miller E.A. Yount P.O. Box 210 Cumberland, MD 21501
1	Hercules, Inc. Bacchus Works ATTN: K.P. McCarty P.O. Box 98 Magna, UT 84044
1	Honeywell, Inc. Government and Aerospace Products ATTN: D.E. Broden/ MS MN50-2000 600 2nd Street NE Hopkins, MN 55343
1	IBM Corporation ATTN: A.C. Tam Research Division 5600 Cottle Road San Jose, CA 95193
1	IIT Research Institute ATTN: R.F. Remaly 10 West 35th Street Chicago, IL 60616
2	Director Lawrence Livermore National Laboratory ATTN: C. Westbrook M. Costantino P.O. Box 808 Livermore, CA 94550

DISTRIBUTION LIST

No. Of Copies	Organization
1	Lockheed Missiles & Space Co. ATTN: George Lo 3251 Hanover Street Dept. 52-35/B204/2 Palo Alto, CA 94304
1	Los Alamos National Lab ATTN: B. Nichols T7, MS-B284 P.O. Box 1663 Los Alamos, NM 87545
1	Olin Corporation Smokeless Powder Operations ATTN: V. McDonald P.O. Box 222 St. Marks, FL 32355
1	Paul Gough Associates, Inc. ATTN: P.S. Gough 1048 South Street Portsmouth, NH 03801
2	Princeton Combustion Research Laboratories, Inc. ATTN: M. Summerfield N.A. Messina 475 US Highway One Monmouth Junction, NJ 08852
1	Hughes Aircraft Company ATTN: T.E. Ward 8433 Fallbrook Avenue Canoga Park, CA 91303
1	Rockwell International Corp. Rocketdyne Division ATTN: J.E. Flanagan/HB02 6633 Canoga Avenue Canoga Park, CA 91304
4	Sandia National Laboratories Combustion Sciences Dept. ATTN: R. Cattolica S. Johnston P. Mattern D. Stephenson Livermore, CA 94550
1	Science Applications, Inc. ATTN: R.B. Edelman 23146 Cumorah Crest Woodland Hills, CA 91364
1	Science Applications, Inc. ATTN: H.S. Pergament 1100 State Road, Bldg. N Princeton, NJ 08540
3	SRI International ATTN: G. Smith D. Crosley D. Golden 333 Ravenswood Avenue Menlo Park, CA 94025
1	Stevens Institute of Tech. Davidson Laboratory ATTN: R. McAlevy, III Hoboken, NJ 07030
1	Teledyne McCormack-Selph ATTN: C. Leveritt 3601 Union Road Hollister, CA 95023
1	Textron, Inc. Bell Aerospace Co. Division ATTN: T.M. Ferger P.O. Box 1 Buffalo, NY 14240
1	Thiokol Corporation Elkton Division ATTN: W.N. Brundige P.O. Box 241 Elkton, MD 21921
1	Thiokol Corporation Huntsville Division ATTN: R. Glick Huntsville, AL 35807
3	Thiokol Corporation Wasatch Division ATTN: S.J. Bennett P.O. Box 524 Brigham City, UT 84302

DISTRIBUTION LIST

No. Of Copies	Organization
1	United Technologies ATTN: A.C. Eckbreth East Hartford, CT 06108
3	United Technologies Corp. Chemical Systems Division ATTN: R.S. Brown T.D. Myers (2 copies) P.O. Box 50015 San Jose, CA 95150-0015
2	United Technologies Corp. ATTN: R.S. Brown R.O. McLaren P.O. Box 358 Sunnyvale, CA 94086
1	Universal Propulsion Company ATTN: H.J. McSpadden Black Canyon Stage 1 Box 1140 Phoenix, AZ 85029
1	Veritay Technology, Inc. ATTN: E.B. Fisher 4845 Millersport Highway P.O. Box 305 East Amherst, NY 14051-0305
1	Brigham Young University Dept. of Chemical Engineering ATTN: M.W. Beckstead Provo, UT 84601
1	California Institute of Tech. Jet Propulsion Laboratory ATTN: MS 125/159 4800 Oak Grove Drive Pasadena, CA 91103
1	California Institute of Technology ATTN: F.E.C. Culick/ MC 301-46 204 Karman Lab. Pasadena, CA 91125
1	University of California, Berkeley Mechanical Engineering Dept. ATTN: J. Daily Berkeley, CA 94720
1	University of California Los Alamos Scientific Lab. ATTN: T.D. Butler P.O. Box 1663, Mail Stop B216 Los Alamos, NM 87545
2	University of California, Santa Barbara Quantum Institute ATTN: K. Schofield M. Steinberg Santa Barbara, CA 93106
1	University of Southern California Dept. of Chemistry ATTN: S. Benson Los Angeles, CA 90007
1	Case Western Reserve Univ. Div. of Aerospace Sciences ATTN: J. Tien Cleveland, OH 44135
1	Cornell University Department of Chemistry ATTN: E. Grant Baker Laboratory Ithaca, NY 14853
1	Univ. of Dayton Rsch Inst. ATTN: D. Campbell AFRPL/PAP Stop 24 Edwards AFB, CA 93523
1	University of Florida Dept. of Chemistry ATTN: J. Winefordner Gainesville, FL 32611

DISTRIBUTION LIST

No. Of Copies	Organization
3	Georgia Institute of Technology School of Aerospace Engineering ATTN: E. Price W.C. Strahle B.T. Zinn Atlanta, GA 30332
1	University of Illinois Dept. of Mech. Eng. ATTN: H. Krier 144MEB, 1206 W. Green St. Urbana, IL 61801
1	Johns Hopkins University/APL Chemical Propulsion Information Agency ATTN: T.W. Christian Johns Hopkins Road Laurel, MD 20707
1	University of Michigan Gas Dynamics Lab Aerospace Engineering Bldg. ATTN: G.M. Faeth Ann Harbor, MI 48109-2140
1	University of Minnesota Dept. of Mechanical Engineering ATTN: E. Fletcher Minneapolis, MN 55455
3	Pennsylvania State University Applied Research Laboratory ATTN: K.K. Kuo H. Palmer M. Micci University Park, PA 16802
1	Polytechnic Institute of NY Graduate Center ATTN: S. Lederman Route 110 Farmingdale, NY 11735
2	Princeton University Forrestal Campus Library ATTN: K. Brezinsky I. Glassman P.O. Box 710 Princeton, NJ 08540
1	Princeton University MAE Dept. ATTN: F.A. Williams Princeton, NJ 08544
1	Purdue University School of Aeronautics and Astronautics ATTN: J.R. Osborn Grissom Hall West Lafayette, IN 47906
2	Purdue University School of Mechanical Engineering ATTN: N.M. Laurendeau S.N.B. Murthy TSPC Chaffee Hall West Lafayette, IN 47906
1	Rensselaer Polytechnic Inst. Dept. of Chemical Engineering ATTN: A. Fontijn Troy, NY 12181
1	Stanford University Dept. of Mechanical Engineering ATTN: R. Hanson Stanford, CA 94305
1	University of Texas Dept. of Chemistry ATTN: W. Gardiner Austin, TX 78712
1	University of Utah Dept. of Chemical Engineering ATTN: G. Flandro Salt Lake City, UT 84112

DISTRIBUTION LIST

No. Of Copies	Organization
1	Virginia Polytechnic Institute and State University ATTN: J.A. Schetz Blacksburg, VA 24061

Aberdeen Proving Ground

Dir, USAMSAA
ATTN: AMXSY-D
AMXSY-MP, H. Cohen
Cdr, USATECOM
ATTN: AMSTE-TO-F
Cdr, CRDC, AMCCOM
ATTN: SMCCR-RSP-A
SMCCR-MU
SMCCR-SPS-IL

USER EVALUATION SHEET/CHANGE OF ADDRESS

This Laboratory undertakes a continuing effort to improve the quality of the reports it publishes. Your comments/answers to the items/questions below will aid us in our efforts.

1. BRL Report Number_____ Date of Report_____

2. Date Report Received_____

3. Does this report satisfy a need? (Comment on purpose, related project, or other area of interest for which the report will be used.)_____

4. How specifically, is the report being used? (Information source, design data, procedure, source of ideas, etc.)_____

5. Has the information in this report led to any quantitative savings as far as man-hours or dollars saved, operating costs avoided or efficiencies achieved, etc? If so, please elaborate._____

6. General Comments. What do you think should be changed to improve future reports? (Indicate changes to organization, technical content, format, etc.)

CURRENT ADDRESS

Name

Organization

Address

City, State, Zip

7. If indicating a Change of Address or Address Correction, please provide the New or Correct Address in Block 6 above and the Old or Incorrect address below.

OLD ADDRESS

Name

Organization

Address

City, State, Zip

(Remove this sheet along the perforation, fold as indicated, staple or tape closed, and mail.)

FOLD HERE

Director
U.S. Army Ballistic Research Laboratory
ATTN: SLCBR-DD-T
Aberdeen Proving Ground, MD 21005-5066

NO POSTAGE
NECESSARY
IF MAILED
IN THE
UNITED STATES

OFFICIAL BUSINESS
PENALTY FOR PRIVATE USE, $300

BUSINESS REPLY MAIL
FIRST CLASS PERMIT NO 12062 WASHINGTON, DC
POSTAGE WILL BE PAID BY DEPARTMENT OF THE ARMY

Director
U.S. Army Ballistic Research Laboratory
ATTN: SLCBR-DD-T
Aberdeen Proving Ground, MD 21005-9989

FOLD HERE

END

DTIC

8-86